Electronic Supplementary Material (ESI) for Chemical Communications
This journal is © The Royal Society of Chemistry 2011

Thioamide Quenching of Intrinsic Protein Fluorescence

Jacob M. Goldberg, Rebecca F. Wissner, Alyssa M. Klein & E. James Petersson

Department of Chemistry, University of Pennsylvania
231 South 34th Street, Philadelphia, Pennsylvania 19104-6323 USA.

General Information. Boc-L-thionoleucine-1-(6-nitro)benzotriazolide and Boc-L-thionophenylalanine-1-(6-nitro)benzotriazolide were purchased from Bachem (Torrance, CA). 2-chlorotrityl resin, Fmoc-Ala-OH, Fmoc-Glu(OtBu)-OH, Fmoc-Leu-OH, Fmoc-Arg(Pbf)-OH, Fmoc-Pro-OH, Fmoc-Gly-OH, Fmoc-Val-OH, Fmoc-Phe-OH, Fmoc-Ile(OtBu)-OH, Fmoc-Tyr(OtBu) and Fmoc-Trp(Boc)-OH were purchased from Novabiochem (San Diego, CA). Piperidine and 2-(1*H*-benzotriazol-1-yl)-1,1,3,3-tetramethyluronium hexafluorophosphate (HBTU) were purchased from American Bioanalytical (Natick, MA). Sigmacote®, *N*,*N*-diisopropylethylamine (DIPEA), hen egg-white lysozyme, and phenyl-sepharose CL-4B resin were purchased from Sigma-Aldrich (St. Louis, MO). *E. coli* BL21(DE3) cells and a QuickChange® site-directed mutagenesis kit were purchased from Stratagene (La Jolla, CA). DNA oligomers were purchased from Integrated DNA Technologies, Inc (Coralville, IA). All other reagents were purchased from Fisher Scientific (Pittsburgh, PA). Milli-Q filtered (18 MΩ) water was used for all aqueous solutions (Millipore; Billerica, MA). All peptide synthesis reaction vessels (RVs) were treated with Sigmacote® prior to use. DNA sequencing was performed at the University of Pennsylvania DNA sequencing facility. Matrix-assisted laser desorption ionization (MALDI) mass spectra were collected with a Bruker Ultraflex III MALDI-TOF-TOF mass spectrometer (Billerica, MA). UV absorbance spectra were obtained with a Hewlett-Packard 8452A diode array spectrophotometer (currently Agilent Technologies; Santa

This journal is © The Royal Society of Chemistry 2011

Clara, CA). Fluorescence spectra were collected with a Varian Cary Eclipse fluorescence spectrophotometer fitted with a Peltier multicell holder (currently Agilent Technologies; Santa Clara, CA). Circular dichroism experiments were conducted with an Aviv 410 CD spectrometer (Aviv Biomedical; Lakewood, NJ).

Peptide Synthesis and Purification. Leu-Pro$_2$-Trp (LP_2W) and Leu-Pro$_2$-Tyr (LP_2Y) were each synthesized on a 12.5 μmol scale on 2-chlorotrityl resin. For each synthesis, 2-chlorotrityl chloride resin (100-200 mesh; 0.6 mmol substitution/g; 12.5 μmol) was added to a dry glass RV. The resin was swollen by two successive 15 min incubations with 5 mL dimethylformamide (DMF) and magnetic stirring. After swelling, DMF was removed with vacuum suction and Fmoc-Trp(Boc)-OH or Fmoc-Tyr(OtBu)-OH was coupled to the resin. The amino acid in DMF (5 equiv; 42 mM, 1.5 mL) and DIPEA (10 equiv; 22 μL) were added to the RV and the mixture was allowed to react for 30 min with magnetic stirring. Spent solution was removed with vacuum suction and the resin beads were washed thoroughly with DMF. Excess DMF was removed with vacuum suction and the resin beads were deprotected by treatment with 20% piperidine in DMF (5 mL) for 20 min with magnetic stirring. The deprotection solution was drained from the RV and the beads were rinsed extensively with DMF. Subsequent amino acid couplings and deprotections proceeded as described above, with the exception that the remaining Fmoc-protected amino acids were activated with HBTU (5 equiv) prior to addition to each reaction. The N-terminal Fmoc group was removed before the peptide was cleaved from the resin. After the beads were washed extensively with DMF and dried with CH_2Cl_2, peptides were cleaved by successive 60 min and 30 min incubations on a rotisserie with 2.5 mL of a fresh cleavage cocktail of trifluoroacetic acid (TFA), water, and triisopropylsilane (TIPS) (10:9:1 v/v). After each treatment, the resulting solution was expelled from the RV with nitrogen and reduced

This journal is © The Royal Society of Chemistry 2011

to a volume of less than 1 mL by rotary evaporation. The combined residue was diluted with 6 mL of CH_3CN/H_2O (2:1 v/v).

The peptides were purified by reverse-phase HPLC on a Vydac 218TP C18 semi-prep column (Grace/Vydac; Deerfield, IL) using a linear solvent gradient that ranged from 98% to 60% aqueous phase over 19 min, then to 0% aqueous phase over 5 min, then returning to 98% aqueous phase during a 10 min wash out period. Trp peptides eluted at approximately 23 min with this method and Tyr peptides eluted at approximately 19 min. MALDI-MS was used to confirm identites (Table S1). Purified peptides were dried in a vacuum centrifuge (Savant/Thermo Scientific; Rockford, IL).

Polyproline peptides Leu'-Pro_n-Trp (L'P_nW), n = 2-11, and Leu'-Pro_n-Tyr (L'P_nY), n = 2-10 were each synthesized on a 10 μmol scale using a procedure analogous to that described above. These peptides were synthesized from a common pot of resin (100 μmol). After coupling the appropriate number of proline residues, a 10 μmol portion of resin was removed from the RV and transferred to a separate, clean RV for thioleucine coupling. Since the thioleucine was introduced through the pre-activated Boc-L-thionoleucine-1-(6-nitro)benzotriazolide, HBTU was not added for these couplings. As the synthesis progressed, reagents were scaled accordingly. Peptide cleavage, purification, and characterization followed that described above.

The CaM binding peptide pOCNC has the sequence FRRIARLVGVLREFAFR; in the thioamide derivative pOCNC-F_1', the N-terminal phenylalanine is replaced with thiophenylalanine. The general sequence of these peptides is derived from the bOCNCp peptide fragment described by Contessa *et al*. (Sequence: GGFRRIARLVGVLREWAYR).[1] Each peptide was synthesized on a 100 μmol scale using the same general procedures as those described above. Briefly, a peptide consisting of residues R_2-R_{17} was synthesized on a 200 μmol

This journal is © The Royal Society of Chemistry 2011

scale on 2-chlorotrityl resin with 5 equiv amino acid, 10 equiv DIPEA, and 5 equiv HBTU when needed. Before removal of the Fmoc group from R2, the resin beads were divided into 2 equal portions and transferred to clean RVs for the final coupling of either Fmoc-L-Phe-OH or Boc-L-thionophenylalanine-1-(6-nitro)benzotriazolide. After removal of the N-terminal Fmoc group from pOCNC with 20% piperidine, the resin beads were incubated on a rotisserie twice for 60 min with 10 mL portions of fresh TFA/H_2O/TIPS (38:1:1 v/v). The thioamide-containing peptide was cleaved from the resin and deprotected with two successive 60 min incubations of the resin beads with 10 mL portions of fresh TFA/H_2O/TIPS (18:1:1 v/v). After each incubation period, the cleavage cocktail for each peptide was expelled from the RV with nitrogen and dried by rotary evaporation. The residue was diluted to 10 mL with CH_3CN/H_2O (3:2 v/v) before purification. Crude peptides were purified by reverse-phase HPLC with linear solvent gradients that ramped from 98% to 70% aqueous phase over 6 min, then to 56% aqueous phase over 14 min, then to 0% aqueous phase over 5 min, followed by a 10 min wash out period, during which the solvent system returned to 98% aqueous phase. Using this method, the peptides eluted at approximately 19.5 min (Fig. S1). Peptides were analyzed by MALDI-MS (Table S1).

(*S*)-methyl 2-((*S*)-2-amino-4-methylpentanethioamido)propanoate (thioleucylalanine ester) was prepared as described previously.[2]

This journal is © The Royal Society of Chemistry 2011

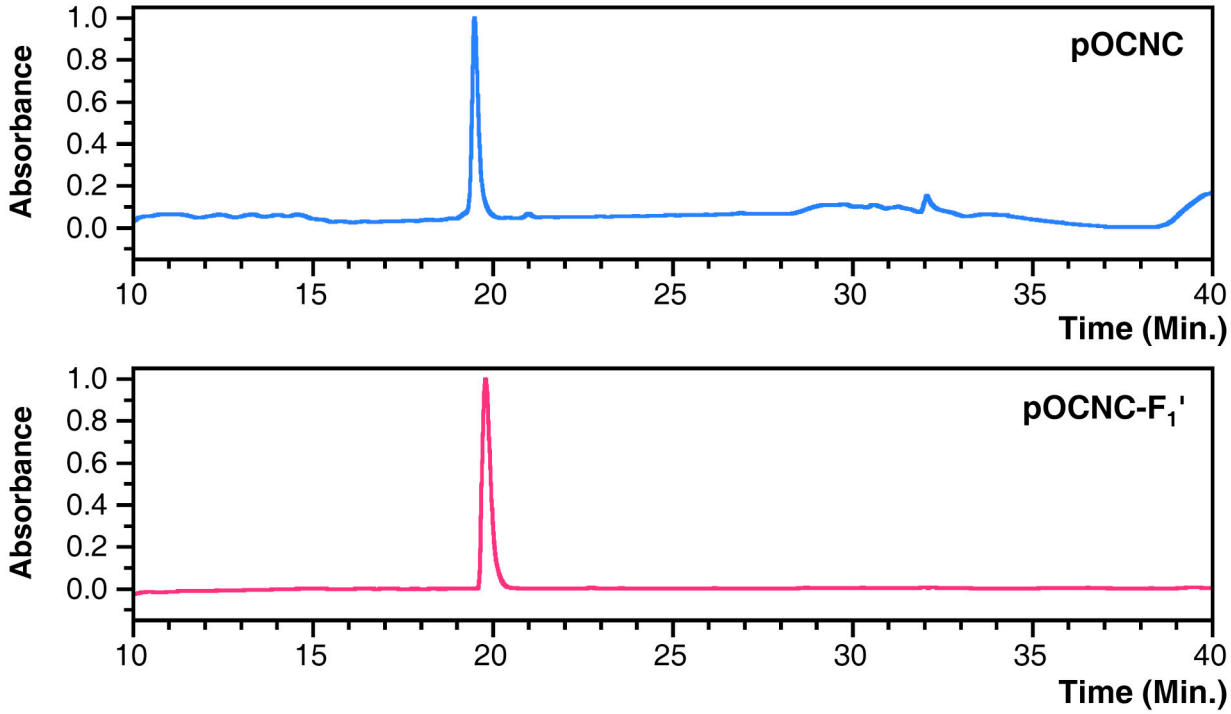

Fig. S1. Analytical HPLC Chromatograms of Purified Peptides. Top: pOCNC monitored at 215 nm. Bottom: pOCNC-F_1' monitored at 277 nm. Absorbance is normalized. Solvent gradients given in text.

This journal is © The Royal Society of Chemistry 2011

Table S1. Calculated and Observed Peptide Masses.

Peptide	Calculated m/z $[M+H]^+$	Observed m/z $[M+H]^+$	Calculated m/z $[M+Na]^+$	Observed m/z $[M+Na]^+$
LP_2Y	489.27	489.15	511.25	511.12
$L'P_2Y$	505.25	505.14	527.23	527.11
$L'P_3Y$	602.30	602.12	624.28	624.08
$L'P_4Y$	699.35	699.16	721.36	721.14
$L'P_5Y$	796.41	796.28	818.39	818.20
$L'P_6Y$	893.46	893.29	915.44	915.27
$L'P_7Y$	990.51	990.21	1012.49	1012.18
$L'P_8Y$	1087.57	1087.24	1109.55	1109.21
$L'P_9Y$	1184.62	1184.60	1206.60	1206.57
$L'P_{10}Y$	1281.67	1281.66	1303.65	1303.66
LP_2W	512.29	512.02	534.27	534.01
$L'P_2W$	528.26	528.28	550.25	550.26
$L'P_3W$	625.32	625.10	647.30	647.07
$L'P_4W$	722.37	722.14	744.35	744.12
$L'P_5W$	819.42	819.33	841.40	841.30
$L'P_6W$	916.48	916.41	938.46	938.39
$L'P_7W$	1013.53	1013.28	1035.51	1035.27
$L'P_8W$	1110.58	1110.27	1132.56	1132.25
$L'P_9W$	1207.63	1207.58	1229.62	1229.51
$L'P_{10}W$	1304.69	1304.57	1326.67	1326.57
$L'P_{11}W$	1401.74	1401.69	1423.72	1423.67
pOCNC	2106.26	2106.78	2128.24	2128.75
pOCNC-F_1'	2122.23	2122.31	2144.22	2144.28

This journal is © The Royal Society of Chemistry 2011

Förster Distance Calculation. The Förster distance, R_0, is given in Å by equation (S1)

$$R_0^6 = \frac{9000(\ln 10)\kappa^2 Q_D J}{128\pi^5 n^4 N_A} \quad \text{(S1)}$$

where κ^2 is a geometrical factor that relates the orientation of the donor and acceptor transition moments, Q_D is the quantum yield of the donor, n is the index of refraction of the solvent, N_A is Avogadro's number, and J is the spectral overlap integral defined in units of $M^{-1}\bullet cm^{-1}\bullet nm^4$.[3] Combining constants and rearranging gives R_0 as

$$R_0 = 0.211\{Q_D \kappa^2 n^{-4} J\}^{1/6} \quad \text{(S2)}$$

J is formally defined as

$$J = \int_0^\infty f_D(\lambda)\varepsilon_A(\lambda)\lambda^4 d\lambda \quad \text{(S3)}$$

where $\varepsilon_A(\lambda)$ is the molar extinction coefficient of the acceptor at each wavelength λ and $f_D(\lambda)$ is the normalized donor emission spectrum given by

$$f_D(\lambda) = \frac{F_{D\lambda}(\lambda)}{\int_0^\infty F_{D\lambda}(\lambda) d\lambda} \quad \text{(S4)}$$

where $F_{D\lambda}(\lambda)$ is the fluorescence of the donor at each wavelength λ. Fluorescence spectra of LP_2W and LP_2Y in water were integrated with KaleidaGraph (Synergy Software; Reading, PA) from 300 to 450 nm for LP_2W and 280 to 400 nm for LP_2Y to calculate $f_D(\lambda)$. UV-Vis spectra of thioleucylalanine ester in water were used to determine $\varepsilon_A(\lambda)$. The literature value of ε_{273} = 12,400 $M^{-1}\bullet cm^{-1}$ was used to prepare solutions of known concentration.[4] J was calculated to be 1.63×10^9 $M^{-1}\bullet cm^{-1}\bullet nm^4$ for the Trp/thioamide pair and 2.21×10^{12} $M^{-1}\bullet cm^{-1}\bullet nm^4$ for the Tyr/thioamide pair. Substituting these results into equation (S2), as well as the quantum yields (0.13 for Trp and 0.14 for Tyr),[5] 1.33 for the index of refraction of water, and 2/3 for κ^2 gives Förster distances of 4.0 Å for the Trp-thioamide pair and 13.4 Å for the Tyr-thioamide pair.

This journal is © The Royal Society of Chemistry 2011

Fluorescence Spectroscopy. Dry proline series peptides were brought up in a minimal volume of pH 7.0 phosphate buffer (150 mM NaCl, 10 mM Na_2HPO_4, pH adjusted with HCl). Tryptophan-containing peptides were diluted to concentrations of approximately 10 μM, as determined by absorbance at 280 nm (ε_{280} = 13,270 M^{-1}•cm^{-1} for thioamide-containing peptides; ε_{280} = 5,600 M^{-1}•cm^{-1} for all others). Tyrosine-containing peptides were diluted to concentrations of approximately 20 μM, as determined by absorbance at 274 nm (ε_{274} = 14,420 M^{-1}•cm^{-1} for thioamide-containing peptides; ε_{274} = 1,420 M^{-1}•cm^{-1} for all others). Corrected fluorescence spectra were collected at 25 °C in triplicate for each peptide using quartz fluorometer cells with path lengths of 1.00 cm. For all Trp experiments, the excitation wavelength was 295 nm and emission data was collected from 300 - 500 nm as the average of three scans. For all Tyr experiments, the excitation wavelength was 275 nm and emission data was collected from 280 – 400 nm. For all experiments, the excitation and emission slit widths were 5 nm, the scan rate was 120 nm/min, the averaging time 0.5 s, and the data interval 1.0 nm. Examples of fluorescence spectra and associated UV spectra are shown in Fig. S2.

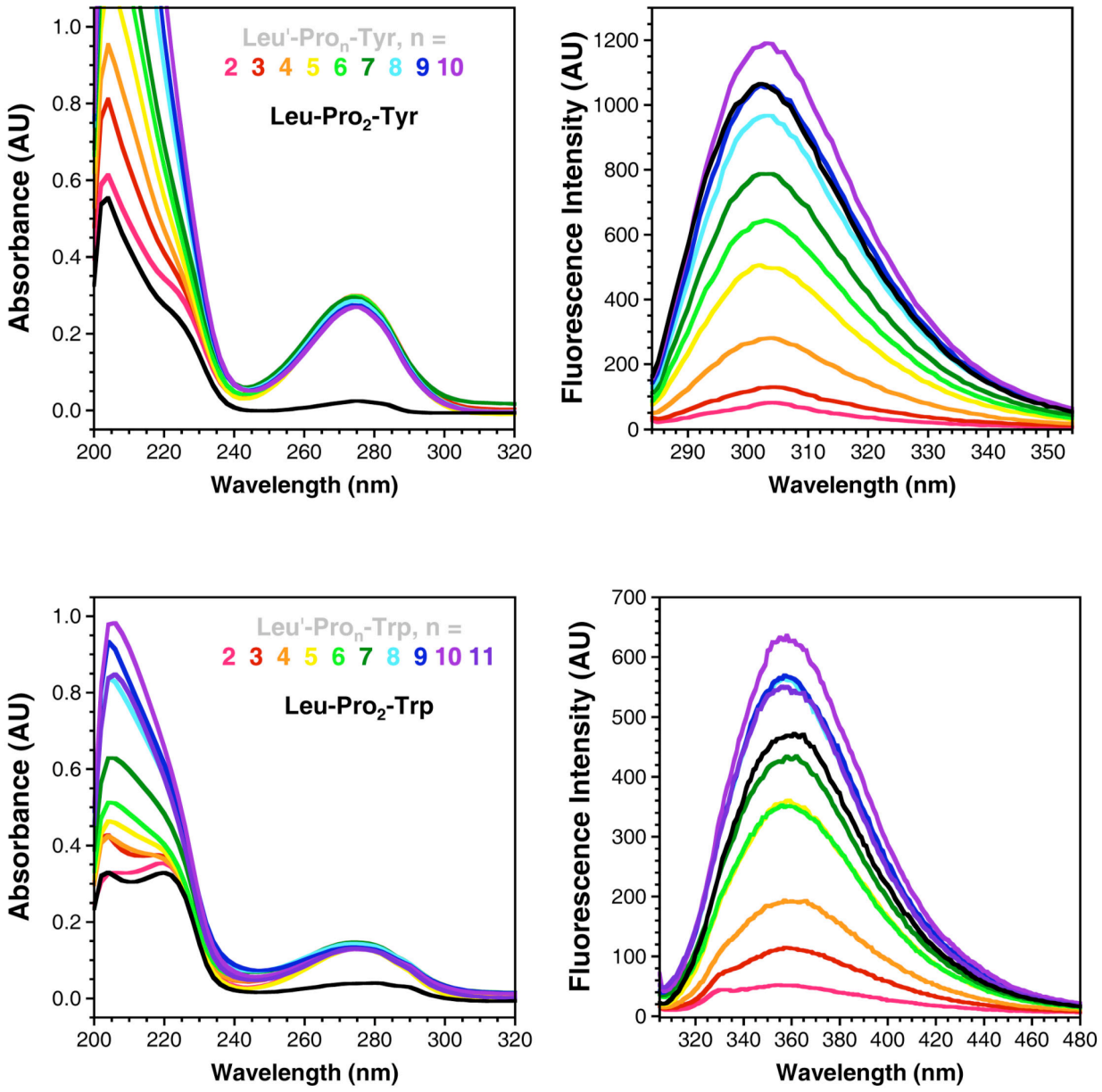

Fig. S2. UV Absorption and Fluorescence Emission Spectra for Pro Series Peptides. Top Left: Tyr UV spectra collected between 200 and 320 nm and background corrected against average absorption from 450 to 500 nm. Top Right: Tyr fluorescence emission spectra collected between 285 and 400 nm with excitation at 275 nm. Bottom Left: Trp UV spectra collected between 200 and 320 nm and background corrected against average absorption from 550 to 650 nm. Bottom Right: Trp fluorescence emission spectra collected between 305 and 480 nm with excitation at 295 nm. Emission spectra colored according to corresponding absorption spectrum.

This journal is © The Royal Society of Chemistry 2011

Proline Series Fluorescence. Fluorescence intensities at the wavelength of maximum emission (λ_{max} = 305 nm for Tyr and λ_{max} = 355 nm for Trp) were averaged from three separate trials for each proline peptide, except for L'P_{10}W, which represents six trials. These values were then normalized to the fluorescence intensity of Leu-Pro_2-Trp or Leu-Pro_2-Tyr, as appropriate, and plotted against the number of prolines separating the chromophores and that distance in angstroms (Fig. 2). The resulting data sets were fit to a sigmoidal function $F(x)$:

$$F(x) = c_1 + \frac{c_2 - c_1}{1 + \left(\frac{x}{c_3}\right)^{c_4}} \qquad \text{(S5)}$$

Here, c_1 through c_4 are constants and the variable x is defined with respect to the choice of the abscissa. In Fig. 2, the data were fit to equation (S5) with the independent variable in terms of n, the number of prolines. Using this fit, the distance in prolines at which 50% quenching is observed is 5.17 ± 0.59 prolines for Tyr (R^2 = 0.98) and 4.58 ± 0.79 prolines for Trp (R^2 = 0.98). Fig. S3 shows the fits to the same equation with the independent variable explicitly cast in angstroms. The distance in angstroms at which 50% quenching is observed is 16.2 ± 2.0 Å for Tyr (R^2 = 0.98) and 15.1 ± 3.0 Å for Trp (R^2 = 0.97).

This journal is © The Royal Society of Chemistry 2011

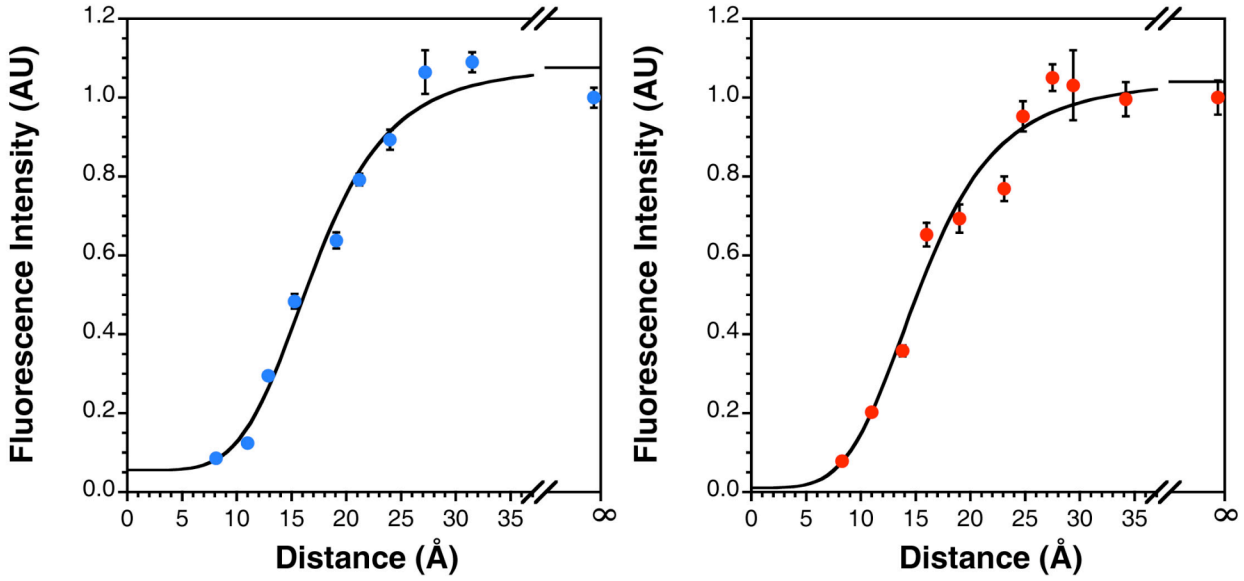

Fig. S3. Fluorescence Intensity as a Function of Interchromophore Distance. Explicit fits of Tyr (left) and Trp (right) fluorescence data from Fig. 2 to equation (S5) with the abscissa in angstroms. Distance calculations described below.

Quenching efficiency (E_Q) as a function of distance in angstroms was calculated using the formula

$$E_Q = 1 - (F/F_0) \qquad \text{(S6)}$$

where F is the fluorescence at each data point and F_0 is taken to be the upper asymptotic limit, c_1. The resulting data sets were plotted against distance in angstroms and fit to equation (S5). Both curves fit the data reasonably well, with goodness-of-fit values of $R^2 = 0.98$ for Tyr and $R^2 = 0.97$ for Trp. Using equation (S5), the distances corresponding to 50% quenching are 16.7 ± 2.2 Å for Tyr and 15.5 ± 3.0 Å, which agree with those values found fitting the raw fluorescence data as described above.

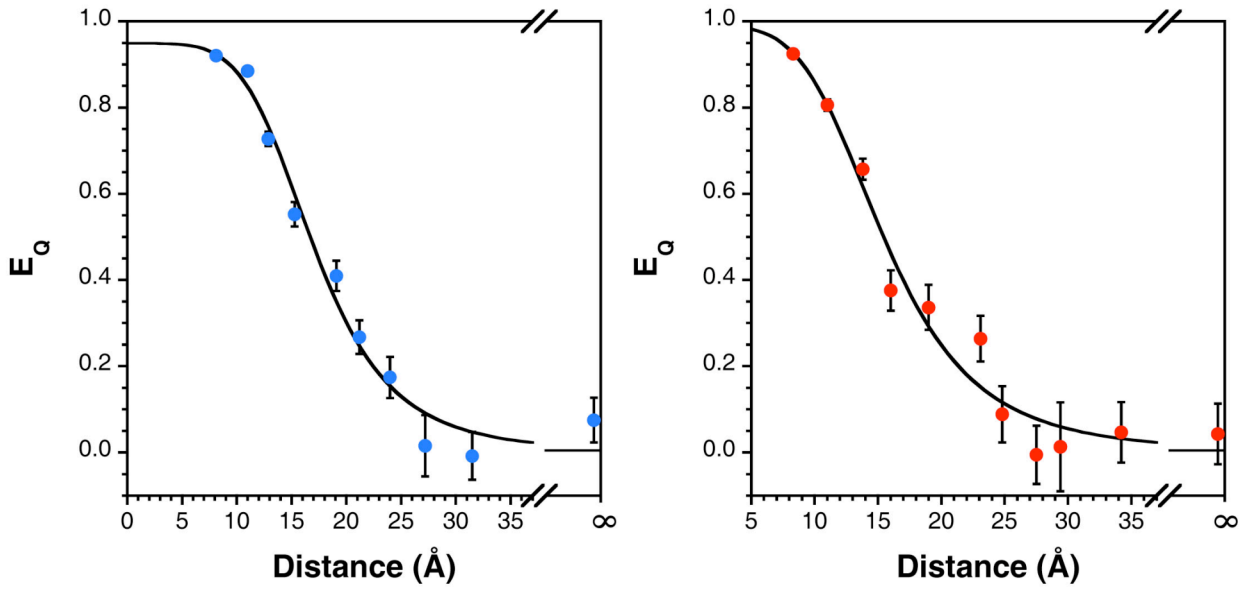

Fig. S4. Quenching Efficiency as a Function of Interchromophore Distance. Thioamide quenching Tyr (left) and Trp (right) fluorescence efficiencies calculated with equation (S6) and fit to equation (S5).

Normalized fluorescence data were also fit to FRET, Dexter, and electron transfer models to evaluate their suitability for describing the observed quenching. For the FRET model, the data were fit to equation (S7) using KaleidaGraph.

$$F = F_0\left\{1 - \frac{1}{1+\left(\frac{R}{R_0}\right)^6}\right\} \qquad \text{(S7)}$$

Here, F_0, the fluorescence of the donor in the absence of the acceptor, and R_0, the Förster distance, are adjustable parameters, and R is the separation between the chromophores in either the number of prolines or the distance in angstroms as calculated from molecular dynamics simulations (described below). Plots of these fits are shown in Fig. S5 as solid traces. Although the curves generally follow the observed pattern of quenching, the values for R_0 that were found to do not agree with those calculated from theory. For example, R_0 was calculated to be 13.4 Å for the Tyr-thioamide pair and was found to be 16.6 ± 0.6 Å experimentally, assuming a FRET

This journal is © The Royal Society of Chemistry 2011

model. For the case of a Trp-thioamide FRET pair, we predicted R_0 to be 4.0 Å, but found a value of 15.3 ± 0.6 Å experimentally.

The data sets were also fit to a Dexter model (equation S8) using KaleidaGraph.[6]

$$F = F_0\left\{1 - \frac{1}{1 + k\exp\left(\frac{2R}{L_{Dex}}\right)}\right\} \qquad \text{(S8)}$$

Here F_0, k, and L_{Dex} (taken to be the sum of the chromophore radii) are adjustable parameters, and R is again the interchromophore separation in number of prolines or distance in angstroms.[7] Values of 7.64 ± 0.84 Å (R^2 = 0.99) and 7.38 ± 1.02 Å (R^2 = 0.98) were found for L_{Dex} for Tyr and Trp, respectively. These values are in relatively close agreement with those predicted by quantum mechanical calculations: 7.16 Å for Tyr/thioamide and 7.44 Å for Trp/thioamide (see below for description of distance determination).

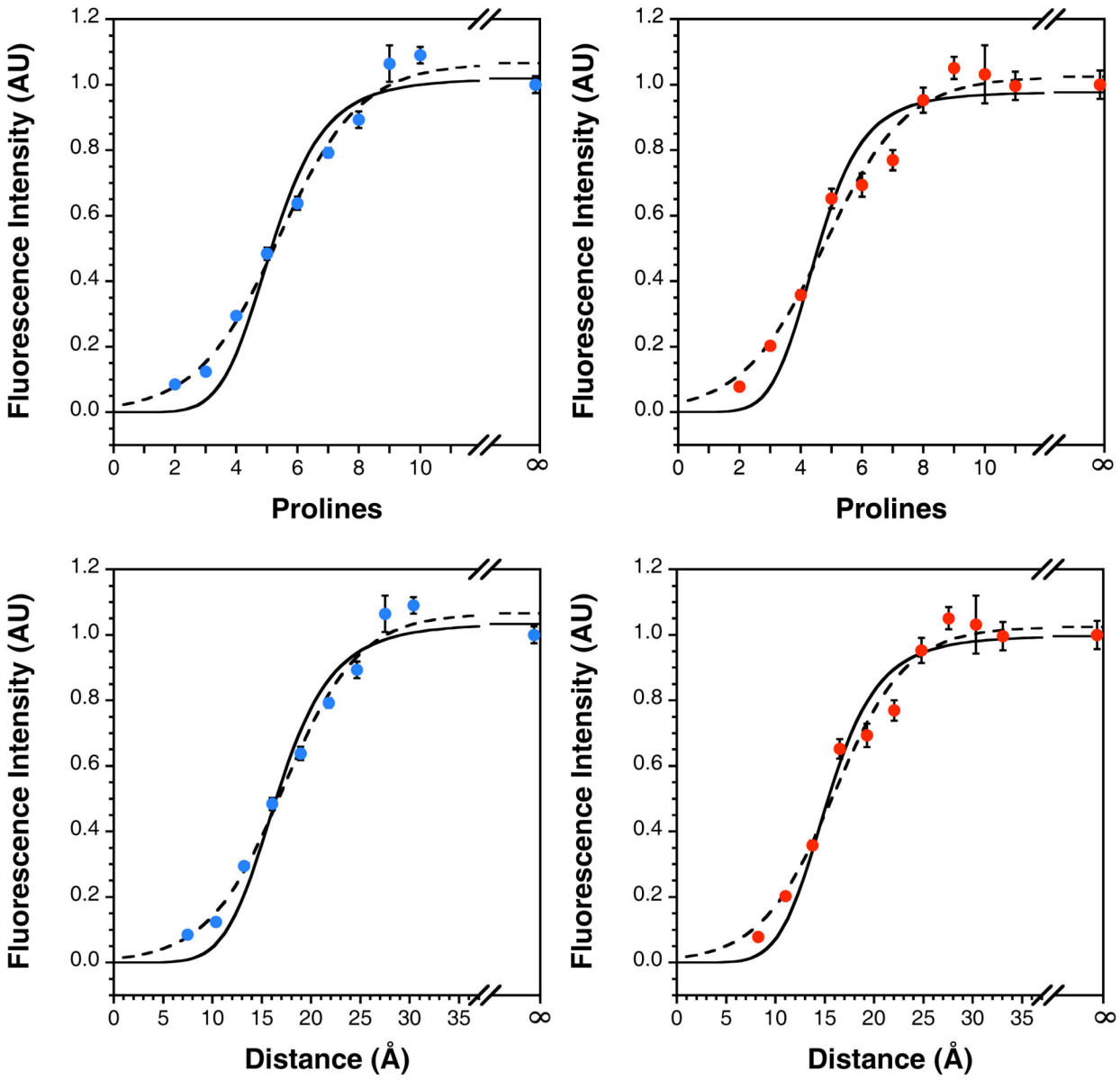

Fig. S5. Fluorescence Intensity Fit to FRET and Dexter Models. Tyrosine (left) and tryptophan (right) fluorescence data from Fig. 2 fit to a FRET model (solid trace) or a Dexter model (dashed trace) with respect to chromophore separation in number of prolines (top) or distance in angstroms (bottom).

Fluorescence intensities were then converted to E_Q according to equation (S6). The quenching efficiencies were fit to each model using equation (S9) for FRET and equation (S10) for Dexter.

$$E_Q = \frac{1}{1+\left(\frac{R}{R_0}\right)^6} \qquad \text{(S9)}$$

This journal is © The Royal Society of Chemistry 2011

$$E_Q = \frac{1}{1 + k\exp\left(\frac{2R}{L_{Dex}}\right)} \quad \text{(S10)}$$

In each case, the values for F_0 obtained from the corresponding distance-in-angstroms plots were used to compute quenching efficiency. Using this method, R_0 was found to be 16.2 ± 0.5 Å (R^2 = 0.96) for the Tyr-thioamide pair and 15.1 ± 0.5 Å (R^2 = 0.95) for the Trp-thioamide pair. Again, these values are larger than those predicted by Förster theory. For the Dexter model, L_{Dex} was found to be 7.6 ± 0.7 Å (R^2 = 0.98) for the Tyr-thioamide pair and 7.5 ± 1.0 Å (R^2 = 0.96) for the Trp-thioamide pair.

Finally, the data were also fit to a general distance-dependent quenching (DDQ) model that has previously been used to describe electron transfer (Fig S7):[5, 8]

$$F = F_0\left\{1 - \frac{1}{1 + k_a\exp\left(\frac{2R - a}{r_e}\right)}\right\} \quad \text{(S11)}$$

In this equation, a is the distance of closest approach of the chromophores, r_e is the so-called characteristic distance, and k_a is the rate of the reaction at the distance a. As before, R is defined as the distance between the chromophores in prolines or angstroms. We note that the form of this equation is similar to that used to describe Dexter transfer, which also has a $1/e^R$ distance dependence. Both data sets were fit to equation (S11). The data were then converted to quenching efficiencies using equation (S6) and fit to equation (S12) with KaleidaGraph (Fig S8).

$$E_Q = \frac{1}{1 + k_a\exp\left(\frac{2R - a}{r_e}\right)} \quad \text{(S12)}$$

Using this equation, r_e was found to be 3.79 ± 2.51 Å for Tyr and 3.75 ± 3.59 Å for Trp in the polyproline ruler system.

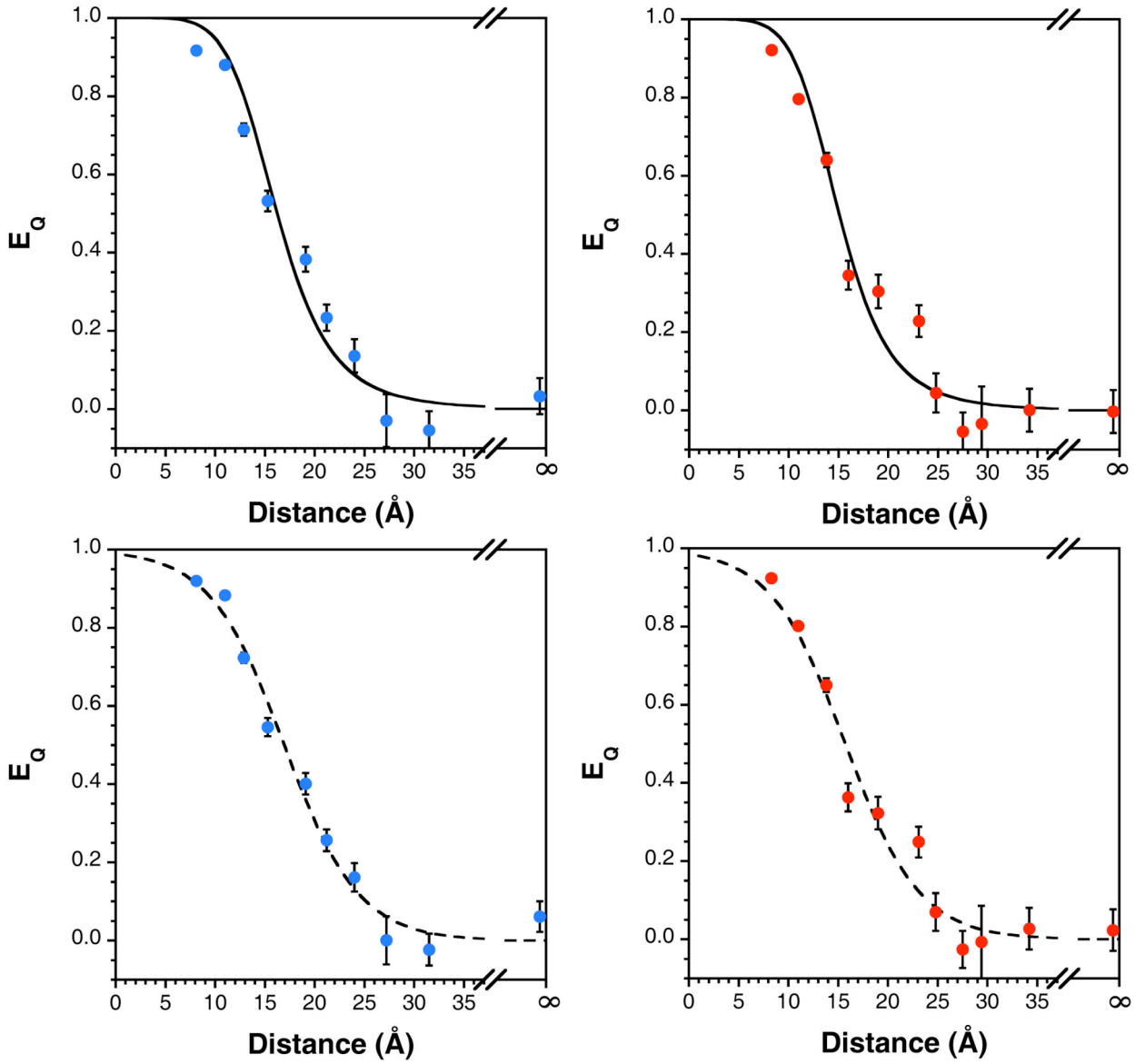

Fig. S6. Proline Series Quenching Efficiency Described by FRET and Dexter Models. Thioamide quenching Tyr (left) and Trp (right) fluorescence efficiencies calculated with equation (S6) and fit to $1/R^6$ distance dependence as described by FRET (Top) or $1/e^R$ distance dependence as described by Dexter transfer (Bottom). Error bars indicate standard error.

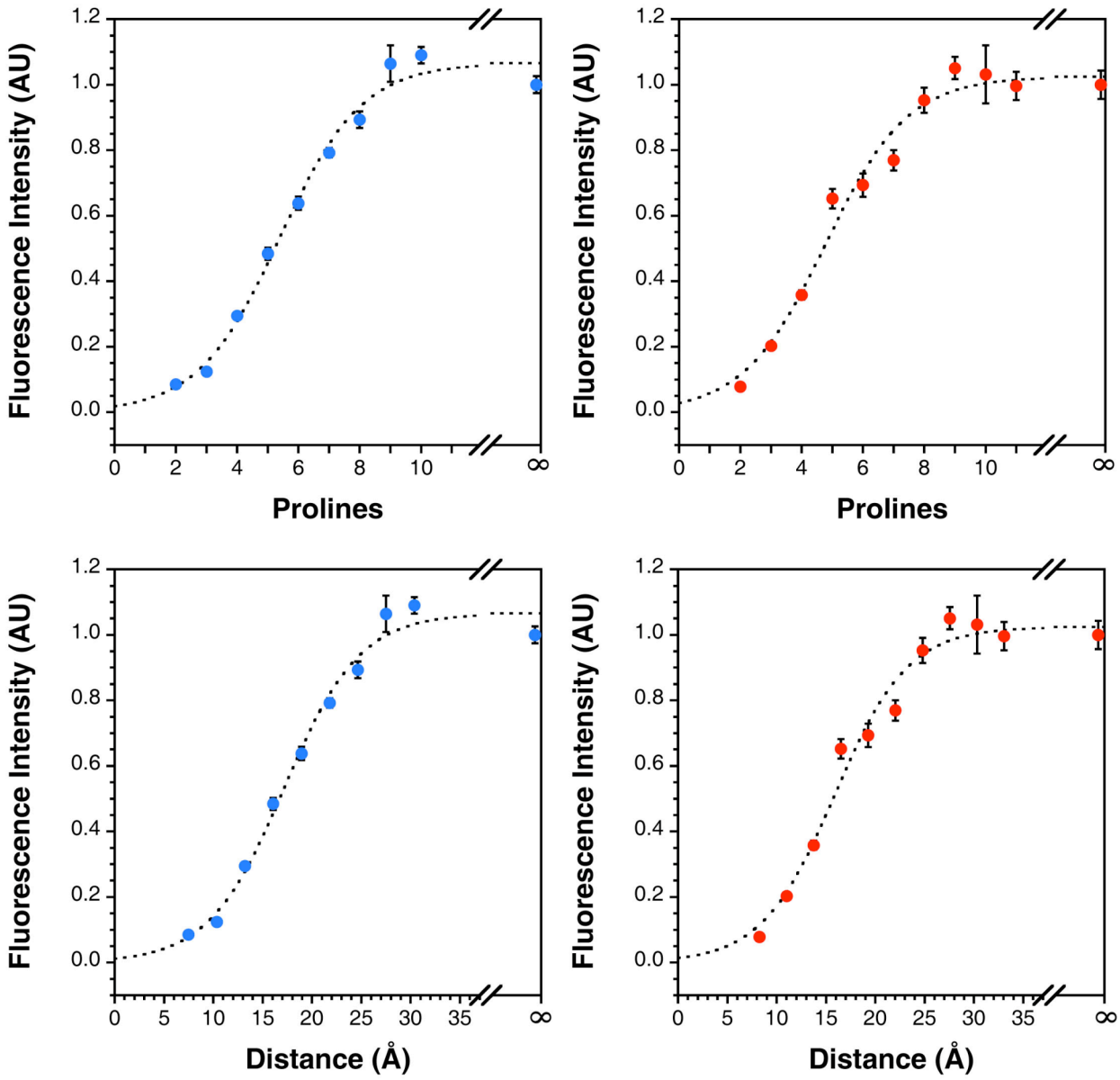

Fig. S7. Proline Series Fluorescence Fit to a DDQ Model. Tyr (left) and Trp (right) fluorescence data from Fig. 2 fit to equation (S11) with the chromophore separation in either number of prolines (Top) or distance in angstroms as determined by molecular dynamics simulations (bottom), described below. Error bars represent standard error.

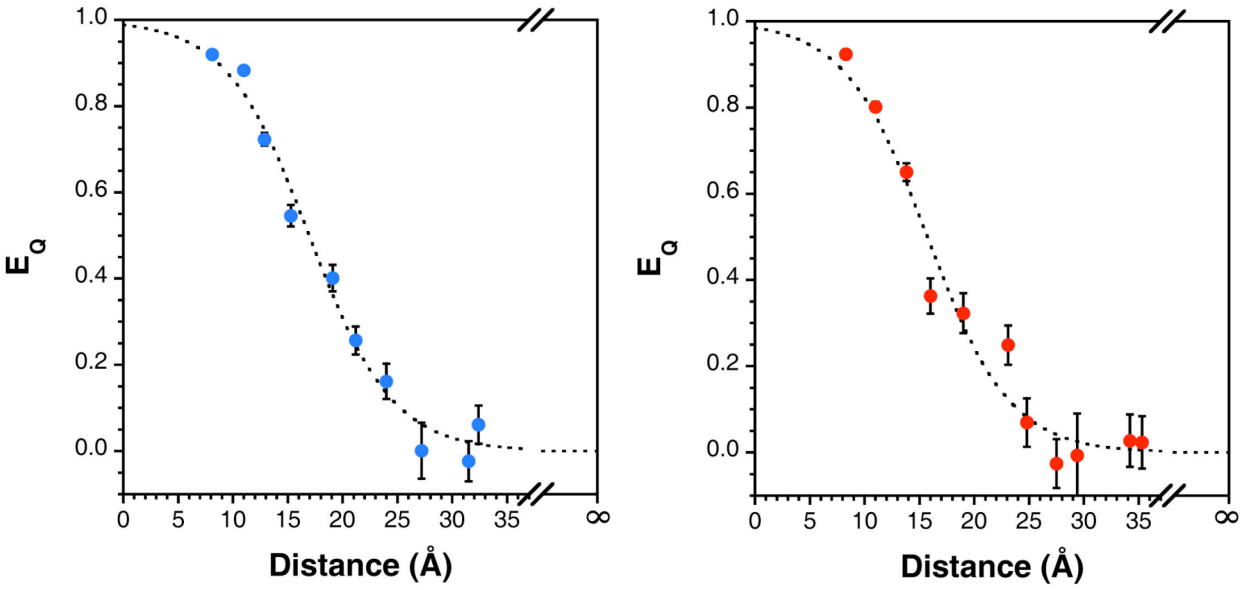

Fig. S8. Proline Series Quenching Efficiency Described by a DDQ Model. Thioamide quenching Tyr (left) and Trp (right) fluorescence efficiencies calculated with equation (S6) and fit to $1/e^{R}$ distance dependence as described by the DDQ model (Equation S12). Error bars indicate standard error.

This journal is © The Royal Society of Chemistry 2011

Molecular Dynamics Calculations: Polyprolines. Starting geometries for 22 proline series peptides (with N-terminal Leu, *C*-terminal Tyr or Trp and n intervening prolines, with n = 2-12) were generated using polyproline type II helix ϕ and ψ angles of - 78° and 149°, respectively. All peptide bonds were initially *trans* (i.e. ω = 180°). *N*- and *C*- termini were left as charged amines and carboxylates, respectively. These were inserted into a TIP3P water box with 10 Å periodic boundaries and no ions. Simulations were performed using the NAMD 2.7b2 package and the CHARMM27 all-atom force field.[9] Covalent bonds involving hydrogen were held rigid using the SHAKE algorithm, allowing a 2 fs time step. A cutoff distance of 12 Å was maintained in calculating nonbonded interactions. Bonded and nonbonded forces were evaluated at every time step, and full electrostatic forces were evaluated at every other time step through application of the particlemesh Ewald (PME) method.[10] The simulation was initiated at 100 K, equilibrated for 25 ps, and warmed to 300 K at a rate of 0.025 K/fs. After warmup, 5 x 10^6 step trajectories (10 ns) were run in the constant temperature and pressure (NPT) ensemble at 300 K.

Chromophore Geometries: Polyprolines. For each 10 ns trajectory, a Tcl script was run in VMD (http://www.ks.uiuc.edu/) to cull distance and orientation information for the leucyl carbonyl and aromatic ring at every tenth timestep over the last 9 ns of the trajectory. The script identified the midpoint between CE1 and CE2 (CEmp) of Tyr or the midpoint between CD2 and CE2 (CDEmp) of Trp. Likewise, the script identified the Leu_1 C as the midpoint of the amide. (Fig. S9) These midpoints serve as convenient anchors that are less sensitive to conformational fluctuations than a single atom position. The interchromophore distance (*R*) was determined as the CEmp-C distance for Leu-Pro_n-Tyr peptides and the CDEmp-Pro_n-C distance for Trp peptides). These distances are shown in Fig. S10, plotted as a function of the number of Pro for the Tyr and Trp series peptides. Data for analogous calculations done on Leu-Pro_n-Phe were reported previously and are also shown in Fig. S10.[2]

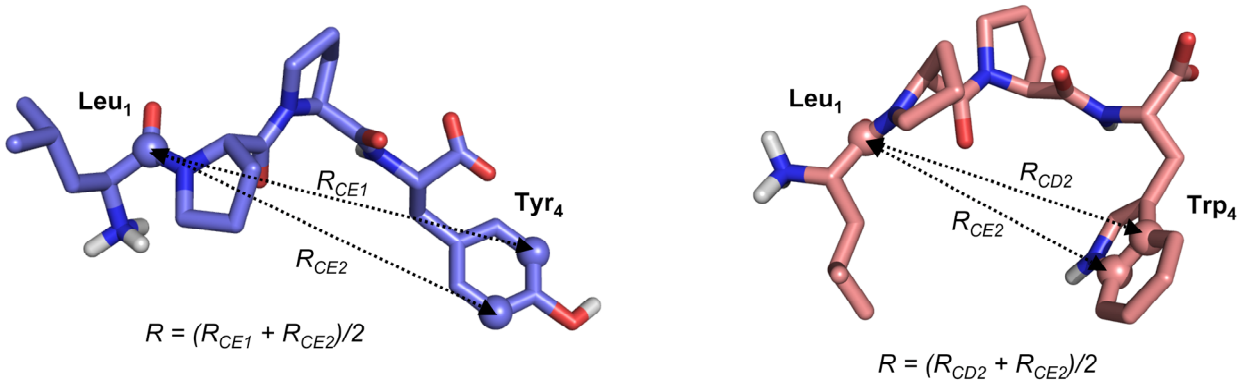

Fig. S9. Interchromophore Distances. Left: Timestep 1 from Leu-Pro$_2$-Tyr simulation shown with atoms used in determining distance (R) illustrated. Right: Timestep 278 from Leu-Pro$_2$-Trp simulation shown with atoms used in determining distance (R) illustrated. Images rendered using PyMOL. (DeLano Scientific, LLC; South San Francisco, CA)

The relationship between chromophore spacing and the number of prolines is relatively linear in all cases, thus a simple linear fit to the data was used to generate the distances in Å used on the abscissa of Fig. 2. These equations (S13, S14, and S15) are listed in Fig. S10.

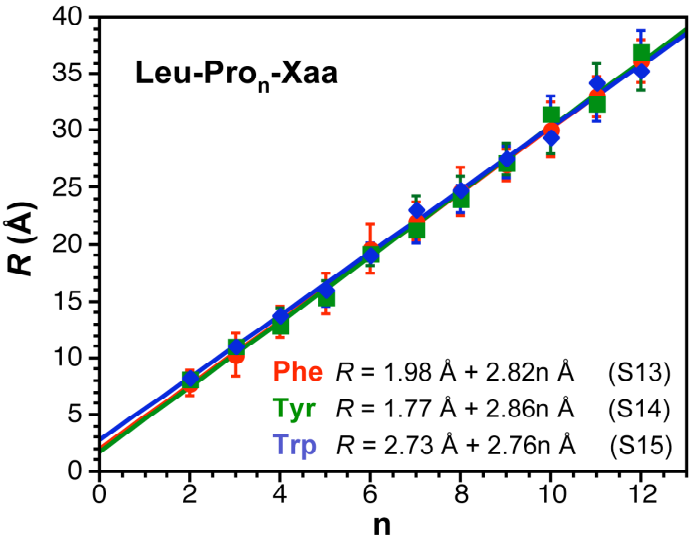

Fig. S10. Interchromophore Distances from MD Simulations. Average distances from last 9 ns of 10 ns simulations of polyproline peptides. Bars indicate RMSD. Equations indicate linear fits to data.

This journal is © The Royal Society of Chemistry 2011

Table S2. Interchromophore Distances Determined from MD Simulations[a]

Pro_2	Tyr	Trp
Average	8.1	8.3
RMSD	1.8	1.7
Pro_3		
Average	11.0	11.0
RMSD	2.4	1.7
Pro_4		
Average	12.9	13.8
RMSD	1.2	1.7
Pro_5		
Average	15.3	16.0
RMSD	1.6	1.4
Pro_6		
Average	19.1	19.0
RMSD	2.1	1.8
Pro_7		
Average	21.2	23.1
RMSD	2.0	2.1
Pro_8		
Average	24.0	24.8
RMSD	1.9	1.3
Pro_9		
Average	27.2	27.5
RMSD	2.0	1.9
Pro_{10}		
Average	31.5	29.4
RMSD	2.6	1.9
Pro_{11}		
Average	32.4	34.2
RMSD	2.0	1.9
Pro_{12}		
Average	37.0	35.3
RMSD	2.1	2.6

[a] Distances (in Å) calculated as described in Supporting Information text.

Quantum Mechanical Calculations. Phenol and indole structures were optimized at the B3LYP level of theory with a 6-311G+ basis set using GAUSSIAN 03 (Gaussian, Inc.; Wallingford, CT).[11] For Dexter fitting, the phenol (Tyr) diameter (d_{Tyr} = 7.38 Å) was computed as the sum of the O12 to C6 distance (4.16 Å) plus the van der Waals radii of oxygen (1.52 Å) and carbon (1.70 Å).[12] The van der Waals radius (R_{Tyr} = 3.69 Å) was computed as one half of this value. The indole (Trp) diameter (d_{Trp} = 7.94 Å) was computed as the sum of the N1 to C8 distance (4.54 Å) plus twice the van der Waals radius of carbon (1.70 Å).[12] The van der Waals radius (R_{Trp} = 3.97 Å) was computed as one half of this value. The thioamide van der Waals radius (R_{SCN} = 3.47 Å) has been reported previously.[2]

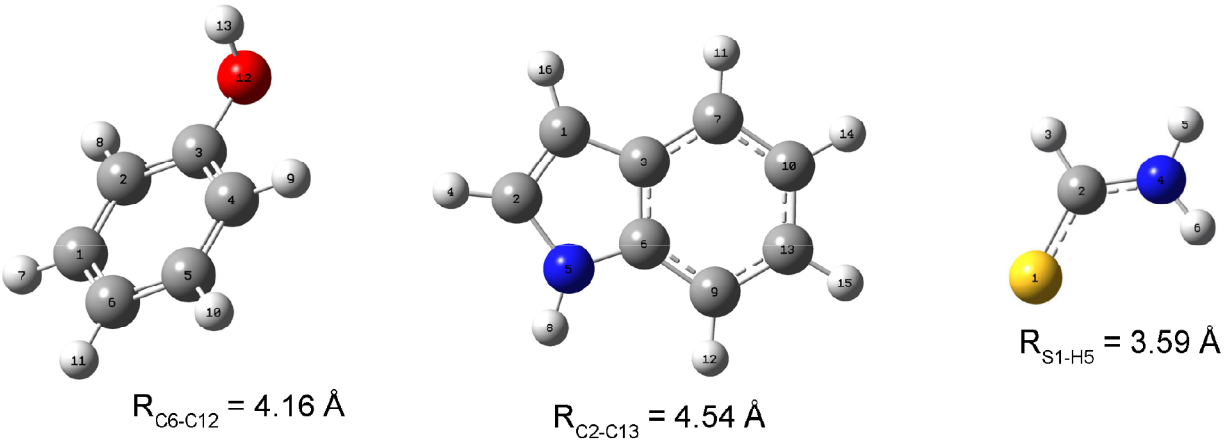

Fig. S11. Chromophore Lengths. B3LYP/6-311G+ minimized geometries for phenol (left), indole (center), and thioformamide (right). Interatomic distances used in calculating chromophore radii are indicated. Fig. rendered using Gaussview 4.1. (Gaussian, Inc.; Wallingford, CT)

Cloning of Calmodulin Expression Constructs. A plasmid containing the wild-type chicken calmodulin (CaM) gene was provided by Joshua Wand from the University of Pennsylvania School of Medicine.[13] An insert containing the CaM gene (458 base pairs from start to stop codon) was cloned into a pET15b vector (Novagen, Gibbstown, NJ) between the NcoI and XhoI cut sites. Quikchange® site-directed mutagenesis was used to generate the following CaM mutants: $Y_{100}F$, $Y_{139}F$, $Y_{100}W$, and $Y_{139}W$. The mutant plasmids were verified by DNA sequencing analysis with a T7 promoter primer.

A. CaM Gene

```
5'-atggctgatcaactgacagaagagcagattgcagaattcaaagaagctttttcactattt
gacaaggatggtgatggtactataactacaaaggagttggggactgtgatgagatcacttggt
cagaaccccacagaagcagaattacaggacatgatcaatgaagtagacgctgatggcaatggc
acaattgacttcccagagtttctgacaatgatggcaagaaaaatgaaagatacagatagcgaa
gaagaaattagagaagcgttccgtgtgtttgacaaggatggtaatggttacattagtgctgca
gaacttcgtcatgtgatgacaaatcttggggagaagctaacagatgaagaagttgatgaaatg
attagggaagcagacattgatggtgatggtcaagtaaactatgaagagtttgtacagatgatg
acagcgaagtga-3'
```

B. Chicken CaM Amino Acid Sequence

```
MADQLTEEQIAEFKEAFSLFDKDGDGTITTKELGTVMRSLGQNPTEAELQDMINEVDADGNGTIDFPEFLTMMARKM
KDTDSEEEIREAFRVFDKDGNGYISAAELRHVMTNLGEKLTDEEVDEMIREADIDGDGQVNYEEFVQMMTAK
```

C. DNA Oligomers used for Quikchange® Mutagenesis

Y100F_For	5'-gacaaggatggtaatggtttcattagtgctgcagaactt-3'
Y100F_Rev	5'-aagttctgcagcactaatgaaaccattaccatccttgtc-3'
Y139F_For	5'-agacattgatggtgatggtcaagtaaactttgaagagtttgtaca-3'
Y139F_Rev	5'-tgtacaaactcttcaaagtttacttgaccatcaccatcaatgtct-3'
Y100W_For	5'-tgacaaggatggtaatggttggattagtgctgcagaacttcg-3'
Y100W_Rev	5'-cgaagttctgcagcactaatccaaccattaccatccttgtca-3'
Y139W_For	5'-tgatggtgatggtcaagtaaactgggaagagtttgtacagatgatgac-3'
Y139W_Rev	5'-gtcatcatctgtacaaactcttcccagtttacttgaccatcaccatca-3'

Fig. S12. A: DNA sequence of chicken CaM gene from start to stop codon. B: Amino acid sequence of chicken CaM. Y_{100} and Y_{139} residues highlighted in red. C: Forward and reverse DNA oligomers used for site-directed mutagenesis.

This journal is © The Royal Society of Chemistry 2011

Protein Expression and Purification. The plasmid containing the chicken CaM gene was used to transform *Escherichia coli* BL21(DE3) cells. Transformed cells were selected on the basis of ampicillin resistance. Single colonies were used to inoculate 50 mL of M9 minimal media supplemented with ampicillin (100 μg/mL). To an autoclaved solution containing 42.3 mM Na_2HPO_4, 22.0 mM KH_2PO_4, and 8.5 mM NaCl, the following autoclaved solutions were added per liter of M9 salts: 10 mL of 10% NH_4Cl, 1 mL of 2 M $MgSO_4$, 1 mL of 15 mg/mL $FeCl_2$ (in 1.0 M HCl), 1 mL of 15 mg/mL $ZnCl_2$ (in acidified H_2O), and 2 mL of 10% Bacto™ Yeast Extract. The primary 50 mL culture was incubated at 37 °C with shaking at 250 rpm overnight. The cells were harvested at 5000 g for 15 min and the resulting pellet was re-suspended in 1 L of M9 minimal media supplemented with ampicillin. The 1 L culture was incubated at 37 °C with shaking at 250 rpm until the absorbance at 600 nm reached 0.9 AU. Protein expression was induced with isopropyl D-galactoside (IPTG), and the culture was incubated at 25 °C for an additional 12 h. The cells were again harvested at 5000 g for 15 minutes and the resulting pellet was suspended in 15 mL of MOPS resuspension buffer: 50 mM 3-(*N*-morpholino)propanesulfonic acid (MOPS), 100 mM KCl, 1 mM ethylenediaminetetraacetic acid (EDTA), 1 mM dithiothreitol, pH 7.5. Cell lysis was achieved by incubating the resuspended cells with lysozyme (150 μg/mL) for 1 h at room temperature followed by brief sonication. Following sonication, the cell lysate was allowed to cool on ice for 5 min. $CaCl_2$ was added to the sonicated lysate to a final concentration of 5 mM prior to centrifugation for 20 minutes at 30,000 g, 4 °C. CaM was purified from the cleared cell lysate using a phenyl-sepharose CL-4B column with EDTA as eluant. Using a total resin bed volume of 20 mL, the column was first equilibrated with 4 column volumes of Buffer A (50 mM Tris base, 1 mM $CaCl_2$, pH 7.5). After the cleared cell lysate was loaded and allowed to pass through the resin, the

column was washed with 4 column volumes of Buffer A, 4 column volumes of high-salt Buffer B (50 mM Tris base, 0.5 M NaCl, 0.1 mM $CaCl_2$, pH 7.5), and an additional 2 column volume washes of Buffer A to restore low-salt conditions. CaM was eluted with Buffer C (10 mM Tris base, 10 mM EDTA, pH 7.5) and collected in 4 mL fractions until absorbance at 280 nm was no longer detected. A second column purification was performed on the first batch of eluted fractions (re-saturated with $CaCl_2$ to a concentration of 20 mM) to obtain CaM with high levels of purity. Column fractions were dialyzed against 10 mM ammonium bicarbonate (pH 8.0) and stored as a lyophilized powder at -20 °C. SDS-PAGE analysis was performed to analyze dialyzed CaM elution fractions.

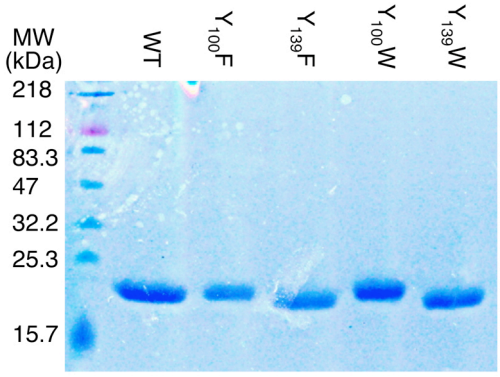

Fig. S13. SDS-PAGE gel of purified CaM mutants. Approximately 10 μM samples denatured at 95 °C in the presence of SDS.

Calmodulin Circular Dichroism Measurements. Mutant stability was evaluated using temperature-dependent circular dichroism (CD) spectroscopy. Since calcium-containing CaM (holo CaM) is thermostable (T_m > 90 °C), we specifically examined the thermal unfolding of the apo protein, for which the reported T_m is 55 °C.[14] To compare the apo and holo forms, purified protein was dialyzed against 2 mM EDTA in 50 mM 4-(2-hydroxyethyl)piperazine-1-ethanesulfonic acid (HEPES) pH 6.70 or 10 mM $CaCl_2$ in 50 mM HEPES pH 6.70. CD data were obtained from approximately 20 μM protein samples diluted in the appropriate buffer

monitoring at 222 nm, between 5 and 95 °C, using the variable temperature module provided with the Aviv 410 CD spectrometer. Data were collected with a 1 °C/min slope, 30 s averaging time, 2 min temperature equilibration, 5 s response, and 1 nm band width. The resulting ellipticity (θ_D) measurements were transformed to molar residue ellipticity values (θ) using

$$\theta = \theta_D/(c\ell n_R) \qquad \text{(S16)}$$

where c is concentration (M), ℓ is the path length (cm), and n_R is the number of residues. To determine fraction folded (f_f) for the apo protein, linear baselines were fit to the low temperature ($\theta_F = m_F T + b_F$) or high temperature ($\theta_U = m_U T + b_U$) data. The full data range was then fit to equation (S17) where $K = e^{-(\Delta H - T\Delta S)/RT}$, ΔH and ΔS are adjustable parameters and R = 8.3145 $J \bullet mol^{-1} \bullet K^{-1}$. Plots are shown for each mutant in Fig. S14.

$$\theta = \theta_F(T)f_f(T) + \theta_u(T)(1 - f_f(T)) \qquad f_f = K/(1+K) \qquad \text{(S17)}$$

Since the holo protein did not melt, only the molar residue ellipticity as a function of temperature is shown for each mutant (Fig. S14).

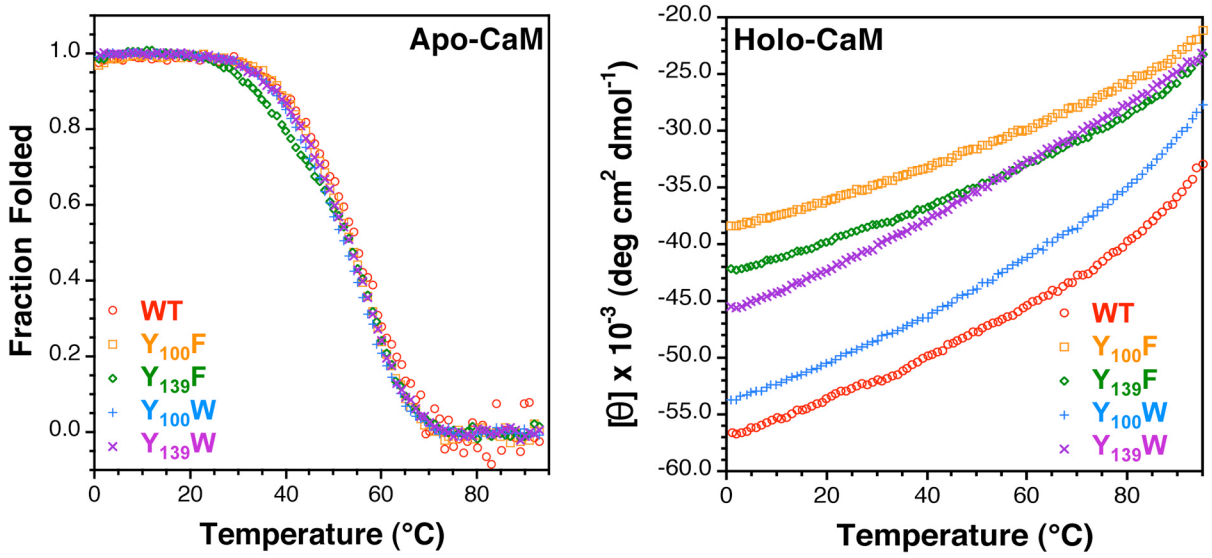

Fig. S14. Temperature-Dependent Circular Dichroism Spectroscopy of Wildtype CaM and Mutants. Left: Fraction folded as a function of temperature as determined by molar residue ellipticity (θ) at 222 nm measured for 20 μM solutions of each protein in the absence of Ca^{2+}. Right: Molar residue ellipticity (θ) at 222 nm measured for 20 μM solutions of each protein in the presence of Ca^{2+}.

This journal is © The Royal Society of Chemistry 2011

Peptide Binding Experiments. All peptide binding experiments were conducted in 15 mM HEPES buffer, 140 mM KCl, and 6 mM $CaCl_2$, pH 6.70. Dry peptides and lyophilized protein were brought up in a minimal amount of buffer to make fresh concentrated stock solutions for each experiment. The absorbance at 280 nm of each protein solution was used to determine its concentration ($\varepsilon_{280,WT}$ = 3000 $M^{-1}\bullet cm^{-1}$; $\varepsilon_{280,Y100F}$ = 1500 $M^{-1}\bullet cm^{-1}$; $\varepsilon_{280,Y139F}$ = 1500 $M^{-1}\bullet cm^{-1}$; $\varepsilon_{280,Y100W}$ = 7400 $M^{-1}\bullet cm^{-1}$; and $\varepsilon_{280,Y139W}$ = 5400 $M^{-1}\bullet cm^{-1}$).[15, 16] For each mutant, solutions were prepared that contained approximately 10 μM protein and a variable amount of peptide, ranging from 0 to approximately 20 μM and representing at least seven distinct concentrations. Each sample was prepared in triplicate using one of two methods. For at least one trial of each mutant, concentrated stocks of protein and peptide were combined with buffer to prepare solutions at each peptide-concentration step. The fluorescence of each solution was measured as described below. For the second trial of each mutant, a sample of protein was diluted to approximately 10 μM in buffer. The fluorescence of this solution was measured as described below and then a concentrated peptide solution of either pOCNC or pOCNC-F_1' was added to obtain a sample that was approximately 20 μM in peptide. The fluorescence of this solution was then recorded and the solution was diluted with 10 μM protein to prepare samples of varying peptide concentration, while maintaining constant protein concentrations. The fluorescence of each sample was measured between dilutions. No variation was observed in the fluorescence of samples prepared by either method. Fluorescence spectra of pOCNC and pOCNC-F_1' were acquired in the absence of protein at each concentration with excitation wavelengths of 275 nm and 295 nm. Essentially no fluorescence was observed exciting the peptides at 295 nm. To confirm that the observed quenching was coming from a peptide binding event, we incubated 10

μM CaM in buffer in the presence and absence of 20 μM thioacetamide and measured the fluorescence by exciting at 275 nm and 295 nm; no change in fluorescence was observed.

Corrected fluorescence measurements as the average of three scans were taken of each sample at 25 °C using quartz fluorometer cells with path lengths of 1.00 cm. For WT, $Y_{100}F$, and $Y_{139}F$ experiments, the excitation wavelength was 275 nm and emission data were collected from 280 - 400 nm. For $Y_{100}W$ and $Y_{139}W$ experiments, the excitation wavelength was 295 nm and emission data were collected from 300 - 500 nm. For all experiments, the excitation and emission slit widths were 5 nm, the scan rate was 120 nm/min, the averaging time 0.5 s, and the data interval 1.0 nm. Representative fluorescence spectra are shown in Fig. S15.

Since pOCNC and pOCNC-F_1' are slightly fluorescent when excited 275 nm (Fig S15), all binding experiment data was background corrected for contributions from peptide fluorescence. The raw signal of the peptide in buffer was subtracted from the raw signal of the protein•peptide complex at each concentration step. These background-corrected values were normalized to the fluorescence of the protein in the absence of peptide (i.e. to the 0 μM sample). The quenching efficiencies listed in Table 1 were estimated from the normalized fluorescence at 1:1 binding stoichiometry.

Predictions of the quenching efficiency for each protein were calculated using our empirical ruler and using Förster theory. The average distance between the thiocarbonyl carbon atom of pOCNC-F_1' and either the ε^1 and ε^2 carbons of Tyr or the δ^2 and ε^2 carbons of Trp were calculated using PyMol from the NMR structure PDB 1SY9.[1] Using this metric the distance between the thioamide and tyrosine was found to be 19.3 Å for Y_{100} and 15.9 Å for Y_{139}. For Trp, the distance was found to be 19.0 Å for W100 and 17.0 Å for W139. Equation (S5) was

This journal is © The Royal Society of Chemistry 2011

used directly to calculate quenching efficiencies at these distances for each of the mutants ($Y_{100}F$, $Y_{139}F$, $Y_{100}W$, and $Y_{139}W$). For the WT protein, we weighted the contribution from each Tyr using the fluorescence sensitivity, which we defined to be the product of the extinction coefficient and the quantum yield (Φ_{Y100} = 0.105; Φ_{Y139} = 0.061) at 275 nm.[17] For Förster calculations, we used equation (S2) and the values of J that we had previously determined from the spectral overlap of thioleucylalanine ester with Trp or Tyr to determine a value of R_0 for each fluorophore. In these calculations, we took κ^2 to be 2/3, approximated n to be 1.33, and substituted the appropriate quantum yield for each donor (Φ_{W100} = 0.15; Φ_{W139} = 0.29).[15] We used these values of R_0 in equation (S9) with the distances inferred from the NMR structure to compute the theoretical quenching efficiency for a FRET mechanism for each mutant. Again, we weighted the quenching efficiency contributions for each Tyr in the wildtype enzyme with their fluorescence sensitivity factors as described above.

The background-corrected, normalized fluorescence data for the titration of pOCNC-F_1' shown if Fig. 3 was fit to equation (S18) using KaleidaGraph.

$$y = 1 - R\frac{\left(\frac{1}{K_a} + [P]_0 + [P]_0[L]_0\right) - \sqrt{\left(\frac{1}{K_a} + [P]_0 + [P]_0[L]_0\right)^2 - 4[P]_0^2[L]_0}}{2[P]_0} \qquad \text{(S18)}$$

Here we define $[L]_0$ and $[P]_0$ to be the total concentration of peptide and protein, respectively.[18] K_a is the equilibrium constant for the peptide binding to the protein to form a 1:1 protein-peptide complex and R is an instrumental response parameter. K_a and R are adjustable parameters in the fit.

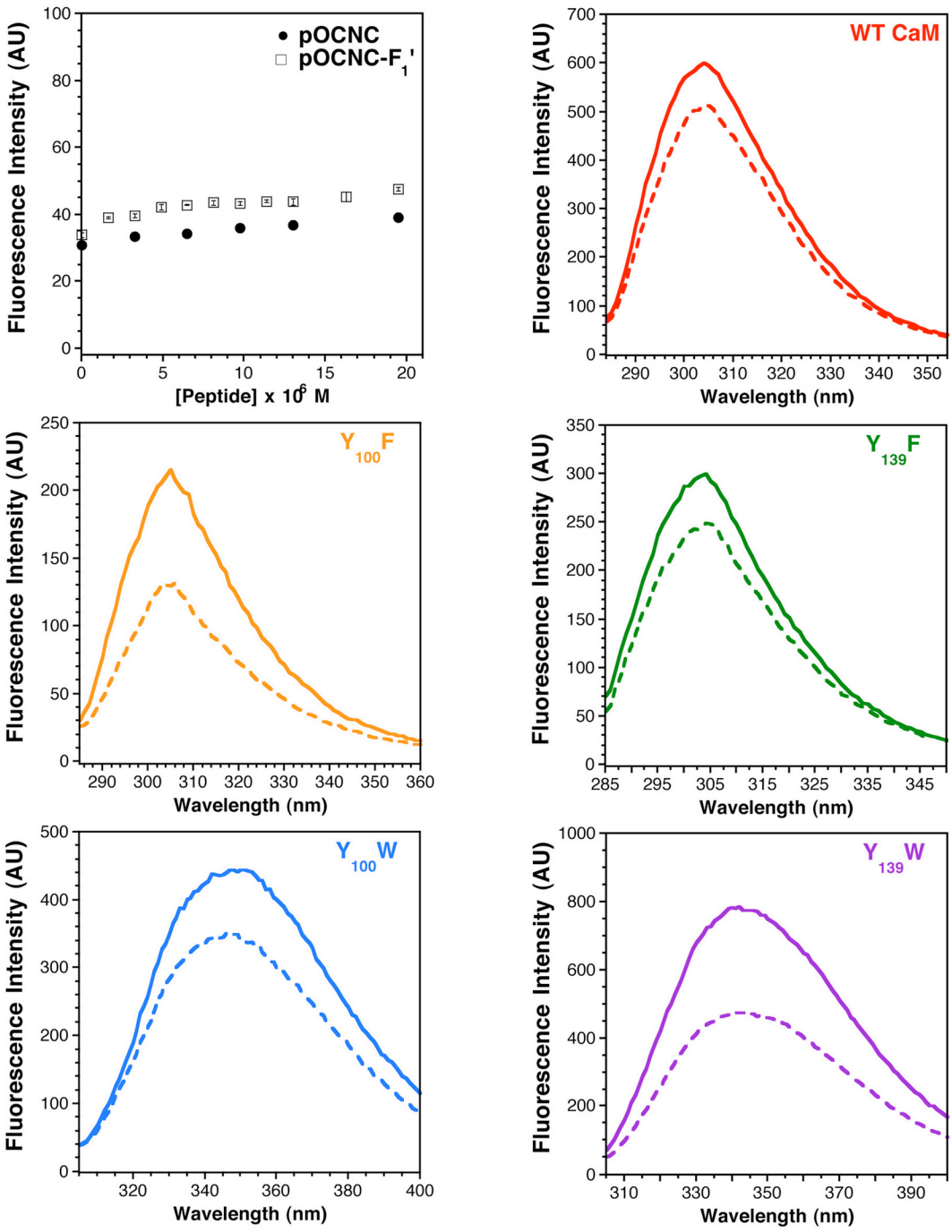

Fig. S15. Representative Fluorescence Spectra of CaM Mutants. Top Left: Fluorescence of pOCNC (circles) and pOCNC-F_1' (squares) as a function of peptide concentration in buffer (ex. 275 nm; em. 305 nm). Top Right: Emission spectra of 10 μM WT CaM in the presence (dashed trace) and absence (solid trace) of 13 μM pOCNC-F_1' (ex. 275 nm). Center: Emission spectra of 8.5 μM Phe mutants with (dashed) and without (solid) 13 μM pOCNC-F_1' (ex. 275 nm). Bottom Left: Emission spectra of 9.4 μM $Y_{100}W$ CaM with (dashed) and without (solid) 13 μM pOCNC-F_1' (ex. 295 nm). Bottom Right: Emission spectra of 13 μM $Y_{139}W$ CaM with (dashed) or without (solid) of 13 μM pOCNC-F_1' (ex. 295 nm).

References

1 G. M. Contessa, M. Orsale, S. Melino, V. Torre, M. Paci, A. Desideri and D. O. Cicero, *J. Biomol. NMR*, 2005, **31**, 185-199.

2 J. M. Goldberg, S. Batjargal and E. J. Petersson, *J. Am. Chem. Soc.*, 2010, **132**, 14718-14720.

3 T. Forster, *Discuss. Faraday Soc.*, 1959, **No. 27**, 7-17;v. d. M. B. W., G. Coker, III and S. S. Y. Chen, *Resonance Energy Transfer: Theory and Data*, Wiley-VCH, New York, NY, 1994.

4 J. Helbing, H. Bregy, J. Bredenbeck, R. Pfister, P. Hamm, R. Huber, J. Wachtveitl, L. De Vico and M. Olivucci, *J. Am. Chem. Soc.*, 2004, **126**, 8823-8834.

5 J. R. Lakowicz, *Principles of fluorescence spectroscopy*, Third edn., Springer, New York, NY, 2006.

6 D. L. Dexter, *J. Chem. Phys.*, 1953, **21**, 836-850.

7 S. Speiser, *Chem. Rev.*, 1996, **96**, 1953-1976.

8 B. Zelent, J. Kusba, I. Gryczynski, M. L. Johnson and J. R. Lakowicz, *J. Phys. Chem.*, 1996, **100**, 18592-18602.

9 L. Kale, R. Skeel, M. Bhandarkar, R. Brunner, A. Gursoy, N. Krawetz, J. Phillips, A. Shinozaki, K. Varadarajan and K. Schulten, *J. Comp. Phys.*, 1999, **151**, 283-312.

10 T. Darden, D. York and L. Pedersen, *J. Chem. Phys.*, 1993, **98**, 10089-10092.

11 M. J. Frisch, G. W. Trucks, H. B. Schlegel, G. E. Scuseria, M. A. Robb, J. R. Cheeseman, J. Montgomery, J. A., T. Vreven, K. N. Kudin, J. C. Burant, J. M. Millam, S. S. Iyengar, J. Tomasi, V. Barone, B. Mennucci, M. Cossi, G. Scalmani, N. Rega, G. A. Petersson, H. Nakatsuji, M. Hada, M. Ehara, K. Toyota, R. Fukuda, J. Hasegawa, M. Ishida, T. Nakajima, Y. Honda, O. Kitao, H. Nakai, M. Klene, X. Li, J. E. Knox, H. P. Hratchian, J. B. Cross, V. Bakken, C. Adamo, J. Jaramillo, R. Gomperts, R. E. Stratmann, O. Yazyev, A. J. Austin, R. Cammi, C. Pomelli, J. W. Ochterski, P. Y. Ayala, K. Morokuma, G. A. Voth, P. Salvador, J. J. Dannenberg, V. G. Zakrzewski, S. Dapprich, A. D. Daniels, M. C. Strain, O. Farkas, D. K. Malick, A. D. Rabuck, K. Raghavachari, J. B. Foresman, J. V. Ortiz, Q. Cui, A. G. Baboul, S. Clifford, J. Cioslowski, B. B. Stefanov, G. Liu, A. Liashenko, P. Piskorz, I. Komaromi, R. L. Martin, D. J. Fox, T. Keith, M. A. Al-Laham, C. Y. Peng, A. Nanayakkara, M. Challacombe, P. M. W. Gill, B. Johnson, W. Chen, M. W. Wong, C. Gonzalez and J. A. Pople, *Gaussian 03*, (1998) Gaussian, Inc., Pittsburgh PA.

12 A. Bondi, *J. Phys. Chem.*, 1964, **68**, 441-451.

13 J. L. Urbauer, J. H. Short, L. K. Dow and A. J. Wand, *Biochemistry*, 1995, **34**, 8099-8109.

14 H. Brzeska, S. V. Venyaminov, Z. Grabarek and W. Drabikowski, *FEBS Lett.*, 1983, **153**, 169-173.

15 J. Haiech and M.-C. Kilhoffer, *Top. Fluoresc. Spectrosc.*, 2000, **6**, 175-209.

16 C. B. Klee, *Biochemistry*, 1977, **16**, 1017-1024.

This journal is © The Royal Society of Chemistry 2011

17 M. C. Kilhoffer, J. G. Demaille and D. Gerard, *Biochemistry*, 1981, **20**, 4407-4414; M. C. Kilhoffer, D. M. Roberts, A. Adibi, D. M. Watterson and J. Haiech, *Biochemistry*, 1989, **28**, 6086-6092.

18 F. H. Stootman, D. M. Fisher, A. Rodger and J. R. Aldrich-Wright, *Analyst*, 2006, **131**, 1145-1151.